Synthesis and Characterization of ZnO Nanoparticles by Thermal Decomposition Method

Ravi Rathore[a)], Disha Harinkhere, and Netram Kaurav[a)]

Department of Physics, Government Holkar Science College, Indore 452001, India.
[a)]Corresponding author: rathore.ravi93@gmail.com, netramkaurav@yahoo.co.uk

Abstract: The paper presents a method for obtaining nanoparticles of ZnO by thermal decomposition of the Zn-containing compounds. The experiment was based on the thermal decomposition of basic Zinc Acetate dihydrate to zinc oxide. Basic Zinc Acetate dihydrate was analysed by derivatography and then annealed at a selected temperature (500 °C to 700°C) for about 3 h. The precursor was decomposed by heating in air resulting in the formation of Hexagonal structure of zinc oxide. Precursor precipitates were transformed into zinc oxide by Thermal decomposition. The precursor and decomposed products were analyzed using XRD analysis and FTIR analysis techniques. The average size of the particles of ZnO obtained using the thermal decomposition technique was approximately 28.8 nm, 34 nm, 39.5 nm at 500 °C, 600 °C, and 700 °C, respectively. FTIR data shows a strong peak at 430 cm^{-1}, assignable to the Zn-O stretching vibrations mode.

INTRODUCTION

ZnO is II-VI group semiconducting material with wide band gap (~3.35eV) and high binding energy (~60meV) at temperature of room which makes it promising material for applications such as photo-detectors, photodiodes, optical modulator waveguides, photodiodes, phosphor material in screens of CRT , gas sensing applications etc. [1-4]. Nanosized ZnO has great potential for being used in formation of solar cells [5], gas sensors [6], chemical absorbent [7] varistors [8], electronic and optical devices [9], electrostatic dissipative lamination [10], catalysts for liquid phase hydrogenation [11], and catalysts for photo-catalytic degradation [12] instead of titanium nanoparticle [13]. The nanoparticles were produced in different conditions of temperature (500°C to 700°C). Fourier transformed infrared spectroscopy (FTIR) and X-ray powder diffractometry (XRD) were used to characterize the nanoparticles composition, their shape, size and crystallinity.

Zinc oxide is not toxic and chemically stable under exposure to both high temperatures and Ultra-Violet. Furthermore, nanoparticles have a large surface area-to-volume ratio that results in a significant increasing of the effectiveness in block of ultra-violet radiation when compared to bulk materials. Several studies on the fabrication of mixed metal oxides containing ZnO have also been reported. The studies were carried out in order to fine-tune ZnO properties for special applications.

Sized-controlled inorganic nanoparticles such as metals, semiconductors, and metal oxide have attracted more interests because of their material properties as comparing with their bulk. Hence, investigations on the synthesis and modification of nanosize ZnO have attracted a lot of attractions. Pure zinc oxide is an insulator and improving its conductivity extends its use to many new applications. Zinc oxide with increased conductivity is suitable for applications where static charge build-up must be prevented. The electrical conductivity can be slightly increased by doping or the introduction of defects into the ZnO crystalline lattice, which can improve the electrical conductivity to the high end for semiconductors.

EXPERIMENTAL PROCEDURE

To obtain ZnO nanoparticles, analytically pure basic Zinc Acetate Dihydrate [$(CH_3COO)_2Zn.2H_2O$] supplied by Merk, was used. To determine the temperature and time of the decomposition of this compound, the sample was annealed at 500°C to 700°C for three hour in a muffle furnace. Then resulting sample cooled up to room temperature. After thermal treatment, the sample was grind for one hour. To identify the crystal structure and chemical composition, the resulting powder was analyzed by X-ray diffraction technique (XRD) and FTIR (Fourier Transform Infrared) measurements. XRD measurements were carried out using Bruker D8 Advance X-rays Diffractometer. The x-rays were produced using a sealed tube and the wavelength of x-ray was 0.154nm (Cu K-alpha). The x-rays were detected using a fast counting detector based on Silicon strip technology (Bruker LynxEye dtector). The crystalline was determined by XRD using a Bruker D8 Advance X-rays Diffractometer equipped with a CuKα (k = 1.54 A °) source (applied voltage 40 kV, current 40 mA). About 0.25 g of the dried particles were deposited as a randomly oriented powder onto a Plexiglass sample container, and the XRD patterns were recorded at angles between 20°and 80°, with a scan rate of 0.5°/min. The sample for IR analysis was prepared by mixing KBr with 10 wt% ZnO powder and then pressing into a pellet at 200 kg cm^{-1} for 1 min.

RESULT AND DISCUSSION

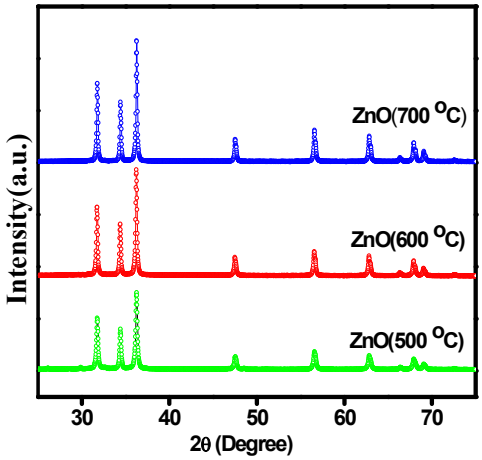

Figure 1. Observed XRD pattern of the ZnO nanoparticles at different temperatures.

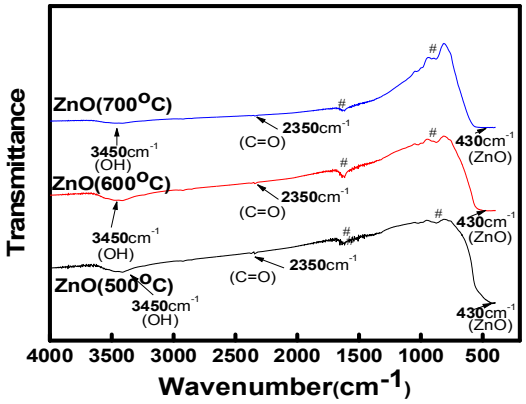

Figure 2. Observed FTIR pattern of the ZnO nanoparticles at different temperatures. (# - residues peaks, probably due to atmospheric moisture and CO_2 respectively).

Figure 1. Shows the XRD patten of ZnO nanoparticles. The figure shows that it is possible to obtain zinc oxide ZnO nanoparticles by thermal decomposition of the zinc compound. The crystallite domain diameters (D) were obtained from XRD peaks according to the Scherrer's equation:

$$D = \frac{k\lambda}{\beta \cos(\theta)}$$

where λ is the wavelength of the incident X-ray beam (1.54 A° for the Cu Kα), θ is the Bragg's diffraction angle, and β is the width of the X-ray pattern line at half peak-height in radians. The average size of the particles of ZnO obtained was approximately 28.8 nm, 34 nm, 39.5 nm at 500 °C, 600 °C, and 700 °C, respectively. Fig. 2 displays the observed FTIR pattern of the ZnO nanoparticles at different temperatures. FTIR data shows a strong peak at 430 cm^{-1}, assignable to the Zn-O stretching vibrations mode. The peaks at 3,450 and 2,350 cm^{-1} indicate the presence of –OH and C=O, residues, probably due to atmospheric moisture and CO_2 respectively [14]. Aggregation between particles when thermal treatment leads to the reduction of the free surface with the secondary elimination of the

grain boundary area via grain growth, thereby disturbing and decreasing the crystal surface energy. With increasing the reaction temperature, the pore volume decreases [20]. In addition, further analysis revealed the effect of the aggregation of isotropic particles on the final shape of the formed ZnO particles. Dispersive forces and electrostatic interparticle attraction is the main factors controlling collection of particles. Isotropic aggregation typically formed spherical particles [21]. The above-mentioned facts can be verified by the fact that irregular particles correspond to the presence of the amorphous fraction at 700 °C, and the particles slightly collapse and form large secondary or tertiary particles. Secondary or tertiary spherical particles at 500 °C and 600 °C stick to each other in random orientation, related to weak vander-Waals forces [22]. With the increase in the calcinations temperature from 500 °C to 600 °C and 700 °C, the average particle size increased.

CONCLUSION

Finally, ZnO nanoparticles were prepared by thermal decomposition at different temperature. It is found that the particle size increases as the sintering temperature increases. Further, the chemical composition of the synthesized materials was then analyzed by FTIR spectroscopy. The spectrum of the material clearly shows the Zn-O absorption band near 430 cm^{-1}.

ACKNOWLEDGMENTS

Financial support from the UGC-DAE CSR, Indore under Collaborative Research Scheme is gratefully acknowledged.

REFERENCES

1. R. H. Bube, Photoconductivity of Solids John Wiley, New York, 404(1967).
2. R. H. Bube, Cambridge University Press, 120(1992).
3. N. Yu, B. Dong, W. W. Yu, B. Hu, Y. Zhang and Yan, Applied Surface Sci. **258**,5729- 5732(2012).
4. C. Wu, X. Qiao, J. Chen, H. Wang, F. Tan and S. Li, Materials Letters **60**,1828-1832(2006) .
5. Z.S. Wang, C.H. Huang, Y.Y. Huang, Y.J. Hou, P.H. XQie, B.W. Zhang and H.M. Cheng, Chem. Mater. **13,** 678(2001).
6. H.M. Lin, S.J. Tzeng, P.J. Hsiau and W.L. Tsai, Nanostruct. Mater. **10,** 465(1998).
7. I. Rosso, C. Galletti, M. Bizzi, G. Saracco and V. Specchia, Ind. Eng. Chem. Res. **42,** 1688(2003).
8. M. Singhal, V. Chhabra, P. Kang and D.O. Shah, Mater. Res. Bull. **32,** 239 (1997).
9. C. Feldmann, Adv. Fundam. Mater. **13,** (2003).
10. M. Kitano and M. Shiojiri, Powder Technol. **93**, 267 (1997).
11. G.M. Hamminga, G. Mul and J.A. Moulijn, Chem. Eng. Sci. **59** (22–23), 5479(2004).
12. M.L. Curridal, R. Comparelli, P.D. Cozzli, G. Mascolo and A. Agostiano, Mater. Sci. Eng. C**23,** 285(2003).
13. G.P. Fotou and S.E. Pratsinis, Chem. Eng. Commum. **151,** 251 (1996).
14. A. Becheri, M. Durr, P.L. Nostro and P. Baglioni, J. Nanopart. Res.10, 679–689(2008).
15. L. Wang and M. Muhammed, J. Mater. Chem. 9, 2871-2878(1999).
16. R. Shankar and R. K. Srivastava, IEEE.13, 978(2013)
17. A. Becheri,M. Durr, P. L. Nostro and P. Baglioni, J. Nanopart. Res. **10**,679–689 (2008).
18. M. S. Niasari, F. Davar, and M. Mazaheri, Materials Letters **62,** 1890–1892 (2008).
19. B. HUTERA, A. KMITA, E. OLEJNIK and T. TOKARSKI, Archives of Metal. and Mater., 58(2013).
20. M. S. Niasari and F. Davar, J. Alloys Compd.**476**, 908-12 (2009).
21. S. J, S. V, B. S and S. L, Powder Technol.**169**, 33–40(2006).
22. K. B. Baharudin, N. Abdullah and D. Derawi, Mater. Res. Express **5,** 125018 (2018).S.C. Zhao and Q M Zhang, Supercond. Sci. Technol. **22**, 015017 (2009).